Homeotropic surface anchoring and the layer-thinning transition in free-standing films

A. A. Canabarro,[1] I. N. de Oliveira,[1,2] and M. L. Lyra[1]
[1]*Instituto de Física, Universidade Federal de Alagoas, 57072-970 Maceió, Alagoas, Brazil*
[2]*Instituto de Física, Universidade de São Paulo, 05315-970 São Paulo, São Paulo, Brazil*
(Received 4 September 2007; published 16 January 2008)

In this work, we investigate the interplay between surface anchoring and finite-size effects on the smectic-isotropic transition in free-standing smectic films. Using an extended McMillan model, we study how a homeotropic anchoring stabilizes the smectic order above the bulk transition temperature. In particular, we determine how the transition temperature depends on the surface ordering and film thickness. We identify a characteristic anchoring for which the transition temperature does not depend on the film thickness. For strong surface ordering, we found that the thickness dependence of the transition temperature can be well represented by a power-law relation. The power-law exponent exhibits a weak dependence on the range of film thicknesses, as well as on the molecular alkyl tail length. Our results reproduce the main experimental findings concerning the layer-thinning transitions in free-standing smectic films.

DOI: 10.1103/PhysRevE.77.011704 PACS number(s): 61.30.Hn, 64.70.M−, 68.35.Md

I. INTRODUCTION

Free-standing smectic films present unusual physical properties which are associated with the interplay of surface and finite-size effects [1,2]. In particular, it has been observed that the surface anchoring can stabilize the smectic order well above the bulk transition temperature [3,4]. As a result, a great variety of phenomena can be observed in thin smectic films, such as wetting transitions [5–7], specific heat anomalies [8,9], and the thickness dependence of the transition temperature [10,11]. As the film thickness may vary from a few nanometers to several micrometers, free-standing films constitute an ideal setup to investigate the crossover from two-dimensional (2D) to three-dimensional behavior.

The wetting phenomenon is a prominent example where the liquid-crystalline surface order exceeds the bulk temperature range, being extensively studied close to nematic–smectic-*A* and isotropic–smectic-*A* phase transitions [5–7,12–14]. Employing x-ray reflectivity [5,7] and optical ellipsometry [15,16] techniques on samples of different homologous series (*n*CB 4–alkyl–cyanobiphenyl, *n*OCB 4–alkyloxy-4–cyanobiphenyl, and $\bar{n}\mathrm{O}.\bar{6}$ 4–hexlyoxphenyl esters of 4–alkyloxybenzoic acid compounds), recent studies have demonstrated that the smectic wetting behavior depends on the alkyl chain length of the liquid crystal compounds. More specifically, it was observed that discrete layering transitions occur in compounds with long alkyl chains, while continuous smectic ordering seems to be favored by the short ones [7,15]. Theoretical and experimental works have demonstrated that the surface anchoring potential plays an important role in the layering and continuous wetting scenarios [12,14,17]. In particular, it was predicted that an enhancement of the surface anchoring can drive a crossover from partial to complete wetting at the isotropic–smectic-*A* transition [13]. Contrasting with the logarithmic divergence of the nematic surface layer at the nematic-isotropic transition [18], the complete wetting of the smectic-*A* phase is characterized by a power-law divergence of the smectic surface phase thickness as the bulk transition temperature is approached [15,19]. This indicates that the long-range nature of surface-surface interactions is relevant in this phenomenon [20–23].

Another interesting and unusual surface-induced phenomenon in free-standing films has attracted great experimental and theoretical interest. This phenomenon is known as the layer-thinning transition. It has been observed in different compounds [24–30] and consists in a stepwise reduction of the film thickness as the temperature is raised above of the bulk transition temperature. X-ray scattering [25] and optical reflectivity [31] measurements have shown that the film thickness reduction is associated with the enhancement of smectic fluctuations in the central layers and the spontaneous formation of dislocation loops. So far, layer-thinning transitions may be described by a simple power-law expression $N(t) \propto t^{-\nu}$, where N is the number of layers and t is the reduced temperature [24]. For different compounds, it was observed that the exponent ν assumes values in the range $0.52 < \nu < 0.82$ [24–30].

Different theories have been used to obtain a qualitative description of the layer-thinning transition [31–34]. Using an extension of the McMillan model [35], Mirantsev proposed that the layer thinning proceeds by the melting of interior layers of the film which squeeze out to the meniscus [33]. For thin films ($N < 13$), this model provides a temperature dependence for the thinning transitions which is in good agreement with the experimental data [24,33]. However, it was reported that the theoretical thinning temperatures were much larger than the experimental values. As a consequence, the asymptotic behavior for thick films approaches the Kelvin law, with $N \propto t^{-1}$, in disagreement with experimental data. Recently, a dislocation model was proposed to explain the mechanism of the layer thinning [31]. In this model, the temperature dependence of the film thickness is obtained from the mean-field divergence of the correlation length ξ. Nevertheless, the layer-thinning transitions were also observed in compounds which exhibit a strong first-order smectic-isotropic transition [36,37]. In this case, the correlation length is expected to stay finite at the transition temperature, even in films under a strong surface anchoring [12].

In this work, we investigate the effects of surface anchoring and finite thickness on the isotropic–smectic-*A* phase

transition in free-standing smectic films. Using an extended McMillan model, we will compute the local nematic and smectic order parameter profiles for films under different strengths of the surface anchoring. The equilibrium profile will be considered to be the one satisfying the self-consistent relations for the nematic and smectic order parameters, which is the global minimum of the Helmholtz free energy. We will be particularly interested in analyzing the transition temperature dependence on the surface anchoring and film thickness. In the context of the layer-thinning transition, we will show that our results are in good agreement with the experimentally proposed power-law relation. The characteristic exponent is also found to slightly depend on the model parameter representing the influence of the molecular structure.

II. EXTENDED MCMILLAN MODEL

A free-standing smectic film consists of a stack of smectic layers confined by a surrounding gas [38]. The film can be considered as a smectic monodomain once the surface interaction induces the molecular alignment to be normal to the layer plane [39]. In a mean-field approach for a film with N discrete layers, the effective potential within the ith smectic layer can be written as [33]

$$V_1(z_1,\theta_1) = -\frac{V_0}{3}[s_1 + s_2 + 3W_0/V_0 + \alpha\cos(2\pi z_1/d)(\sigma_1+\sigma_2)]P_2(\cos\theta_1), \quad (1)$$

$$V_i(z_i,\theta_i) = -\frac{V_0}{3}\left[\sum_{i-1}^{i+1} s_i + \alpha\cos(2\pi z_i/d)\left(\sum_{i-1}^{i+1}\sigma_i\right)\right]P_2(\cos\theta_i), \quad (2)$$

$$V_N(z_N,\theta_N) = -\frac{V_0}{3}[s_N + s_{N-1} + 3W_0/V_0 + \alpha\cos(2\pi z_N/d)(\sigma_N+\sigma_{N-1})P_2(\cos\theta_N). \quad (3)$$

Here, $P_2(\cos\theta_i)$ is the second-order Legendre polynomial with θ_i being the angle in the ith layer between the long axis of the molecule and the z direction. s_i and σ_i are the orientational and translational order parameters in the ith layer, respectively. V_0 is a parameter of the microscopic model [35] that determines the scale of the nematic-isotropic transition temperature. The parameter α is related to the length of alkyl chains of calamitic molecules through the relation $\alpha = 2\exp[-(\pi r_0/d)^2]$, where r_0 is a characteristic length associated with the length of the molecular rigid section and d is the smectic layer spacing. The parameter W_0 corresponds to the strength of the surface anchoring, which is assumed to be short ranged. In particular, W_0 couples with orientational order and represents the surface-induced homeotropic alignment of the director.

The local order parameters s_i and σ_i satisfy the self-consistent equations

$$s_i = \langle P_2(\cos\theta_i)\rangle_i \quad (4)$$

and

$$\sigma_i = \langle P_2(\cos\theta_i)\cos(2\pi z_i/d)\rangle_i, \quad (5)$$

where the thermodynamic averages are computed from the one-particle distribution function in the ith smectic layer,

$$f_i(z_i,\theta_i) \propto \exp(-V_i/k_BT). \quad (6)$$

Here, k_B is the Boltzmann constant and T is the temperature. The order parameter profiles that are solutions of the self-consistent equations (4) and (5) give the extreme value of the total Helmholtz free energy which is formally defined as

$$F = \sum_{i=1}^{N} F_i, \quad (7)$$

where

$$F_1 = n_0V_0\left[\frac{1}{6}s_1(s_1+s_2) + \frac{1}{6}\alpha\sigma_1(\sigma_1+\sigma_2) - \frac{k_BT}{V_0}\ln\left(\frac{1}{d}\int_0^d dz\int_0^1 d(\cos\theta)f_1(z,\cos\theta)\right)\right], \quad (8)$$

$$F_i = n_0V_0\left[\frac{1}{6}s_i\left(\sum_{i-1}^{i+1}s_i\right) + \frac{1}{6}\alpha\sigma_i\left(\sum_{i-1}^{i+1}\sigma_i\right) - \frac{k_BT}{V_0}\ln\left(\frac{1}{d}\int_{(i-1)d}^{id} dz\int_0^1 d(\cos\theta)f_i(z,\cos\theta)\right)\right], \quad (9)$$

$$F_N = n_0V_0\left[\frac{1}{6}s_N(s_{N-1}+s_N) + \frac{1}{6}\alpha\sigma_N(\sigma_{N-1}+\sigma_N) - \frac{k_BT}{V_0}\ln\left(\frac{1}{d}\int_{(N-1)d}^{Nd} dz\int_0^1 d(\cos\theta)f_N(z,\cos\theta)\right)\right]. \quad (10)$$

Here, n_0 is the number of particles in the smectic layers, which is assumed to be constant. From this model, we can obtain the profile of the order parameters for different model parameters. According to the McMillan theory [35], different phase transitions can be observed for typical values of the parameter α. In particular, this model predicts a first-order smectic-isotropic transition for $\alpha \geq 0.98$. In the extended model, it is expected that a strong surface anchoring modifies the McMillan phase diagram, especially in very thin films. On the other hand, the main features of the phase diagram should be unaffected when the film thickness l is much greater than the surface penetration length δ [14]. More specifically, the internal layers of the film should present a similar McMillan phase diagram when $l \gg 2\delta$.

III. THE SMECTIC-ISOTROPIC TRANSITION

A. Melting point and order parameter profiles

In order to investigate the surface anchoring and finite-size effects on the smectic-isotropic phase transition in free-

standing films, we consider the case where $l \gg 2\delta$ and $\alpha > 0.98$. The profile of the order parameters in a film with N layers can be numerically obtained by solving the set of $2N$ self-consistent equations (4) and (5). In this regime, one has a bulk first-order smectic-isotropic transition. In the vicinity of the transition temperature, the self-consistent equations develop three solutions with distinct order parameter profiles, as usual at first-order transitions. One of them corresponds to a global minimum of the free energy and represents the true thermodynamic equilibrium state. A second solution is a local minimum of the free energy, thus being a metastable state that can be reached only through overheating or supercooling processes. The third solution corresponds to an unstable state at which the free energy has a local maximum.

In Ref. [33], the layer-thinning transition was considered to occur at the temperature in which the set of self-consistent equations loses the solution with nonvanishing smectic order on the central layers of an N-layer film. At this point, the film was assumed to thin to the $(N-n)$-layer state having a lower free energy. Based on this mechanism, it was possible to reproduce the power-law temperature dependence of the film thickness only in the regime of very thin films. A strong deviation from the power-law relation was reported to appear for films with $N > 10$, whose origin was conjectured to be related to the use of a mean-field approximation to describe the layer-thinning transition. In what follows, we will show that the procedure used in Ref. [33] overestimated the layer-thinning transition temperature. Actually, a smectic N-layer film becomes metastable at a lower temperature. We will take the temperature at which the smectic film becomes metastable as the transition point to the true equilibrium state corresponding to a thinner film. Within this scenario, the results derived from the extended McMillan mean-field model introduced in Ref. [33] will be shown to display a very good agreement with the experimental findings for a wide range of film thicknesses. This mean-field prescription will also be shown to be able to reproduce the experimentally observed fact that the layer-thinning exponent ν is not unique, which is consistent with a previous phenomenological approach based on the Landau–de Gennes theory [40]. Further, we will report the dependence of the transition temperature on the anchoring energy to reveal the existence of a characteristic surface anchoring strength below which no layer-thinning transition can occur.

Comparing the Helmholtz free energy of the two locally stable solutions, we can determine the order parameter profiles that correspond to the true equilibrium state of the system. In Fig. 1, we show the Helmholtz free energy as a function of temperature for such solutions of the set of self-consistent equations. The model parameters used were $N=25$, $W_0=3.0V_0$, and $\alpha=1.05$, for which the bulk transition temperature is $T_B=0.224\ 82V_0/k_B$. For low enough temperatures, the self-consistent equations have a single solution, with the nematic and smectic order parameters being nonnull along the film, a typical scenario of the smectic phase. In the high-temperature regime, one also has a unique solution. This solution has vanishing order parameters near the film center, i.e., the smectic order has been melted at the central layers. At intermediate temperatures, both kinds of solution

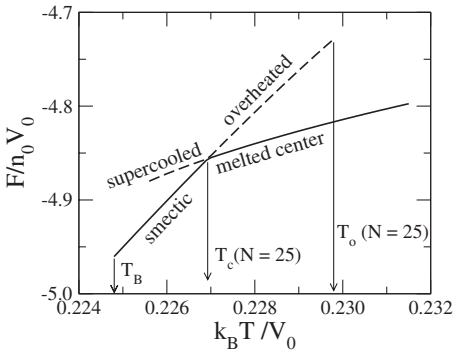

FIG. 1. Helmholtz free energy as a function of temperature for the solutions of the self-consistent equations that are locally stable. The model parameters are $N=25$, $W_0=3.0V_0$, and $\alpha=1.05$. The bulk transition temperature is $T_B=0.224\ 82V_0/k_B$. In the vicinity of the transition temperature $T_c(N=25)=0.226\ 95V_0/k_B$, one can observe the existence of supercooled and overheated solutions (dashed lines). The overheated solution disappears for temperatures above $T_o=0.2298V_0/k_B$. The solid lines represent the equilibrium states.

are locally stable. The temperature at which they have the same free energy defines the transition temperature at which the smectic order starts to melt at the film center. Defining the transition temperature $T_c(N)$ for a film with N layers, we obtain $T_c(N=25)=0.226\ 95V_0/k_B$ for the model parameters mentioned above. This value is well below the value $T_c(N=25)=0.2298V_0/k_B$ previously reported by Mirantsev [33]. Above $T_c(N=25)$, we observe that the solution with a nonnull smectic order at the center of the film corresponds to an overheated smectic phase. In fact, $T=0.2298V_0/k_B$ represents the temperature at which the overheated solution disappears.

In Fig. 2, we present the profile of the order parameters for different values of the temperature. The model parameters are the same as used in Fig. 1. At $T=0.2269V_0/k_B$ [slightly below $T_c(N=25)$], the nematic and smectic order parameters are roughly uniform along the film, except at the outermost layers. Due to the strong surface anchoring, the order parameter profiles present a positive curvature where the surface layers are more ordered than the bulk ones. When $T=0.2270V_0/k_B$ the film center melts, which is signaled by a strong reduction of the nematic and smectic order parameters of the internal layers. In particular, we note that the nematic order parameter is nonuniform along the film, presenting a small, but finite, value in the central layers. In contrast, the smectic order parameter vanishes in the central layers.

In the regime of weak surface anchoring, we can observe profound modifications in the profile of the order parameters near the melting point, as shown in Fig. 3. Here, we used $N=25$, $W_0=0.25V_0$, and $\alpha=1.05$. Now, we notice a reduction in $T_c(N=25)$ which now becomes very close to the bulk transition temperature $(T_B=0.224\ 82V_0/k_B)$. Below $T_c(N=25)$, the profile of the nematic order parameter presents a negative curvature with surface layers being less ordered than the bulk ones. On the other hand, just after the melting point, the nematic order parameter presents a positive curvature which is associated with the homeotropic alignment induced by W_0. In contrast, the surface anchoring is not sufficient to stabilize the smectic order which is null along the

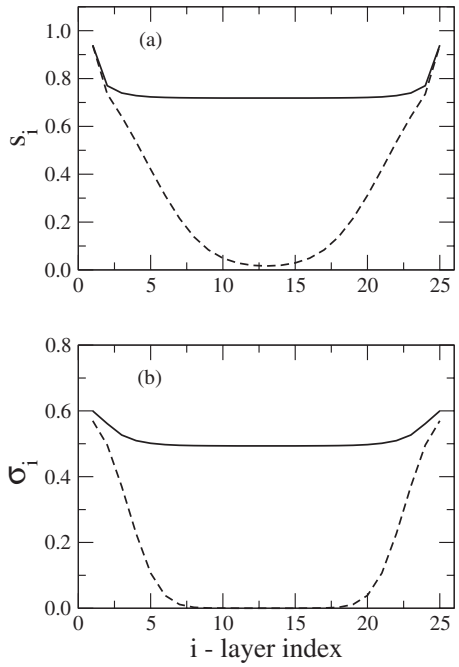

FIG. 2. Profiles of the (a) nematic and (b) smectic order parameters for different temperatures: $T=0.2269V_0/k_B$ (solid lines) and $0.2270V_0/k_B$ (dashed lines). The model parameters are the same used in Fig. 1 (strong anchoring). Notice the discontinuous transition from the state with finite order parameters to the melted state at the film center.

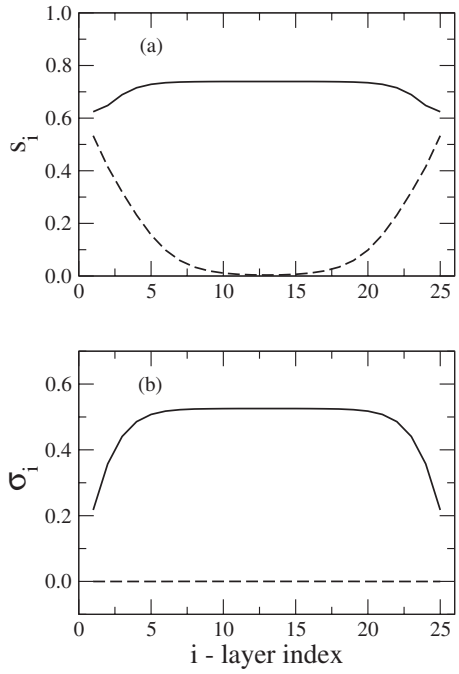

FIG. 3. Profiles of the (a) nematic and (b) smectic order parameters for different temperatures: $T=0.2247V_0/k_B$ (solid lines) and $T=0.224\ 82V_0/k_B$ (dashed lines). The model parameters are $N=25$, $\alpha=1.05$, and $W_0=0.25V_0$ (weak anchoring). Notice that the smectic order melts over the entire film.

whole film. Such behavior is typical for even weaker surface anchoring, except by the fact that the melting temperature of a film with finite thickness becomes slightly below the bulk transition temperature.

In Fig. 4, we present the transition temperature $T_c(N)$ as a function of the surface anchoring for different film thicknesses. Results for two representative values of α are shown. We can notice that $T_c(N)$ increases monotonically as the surface anchoring is enhanced, presenting a finite value in the limit of $W_0/V_0\rightarrow\infty$. It is important to stress that the surface penetration length stays finite at the smectic-isotropic transition. Therefore, $T_c(N)$ approaches the bulk transition temperature as the thickness increases. However, there is a characteristic surface anchoring W_0^* which delimits two qualitatively distinct regimes. Above W_0^* the transition temperature decreases with increasing film thicknesses. This is typical of systems having surface-enhanced order. In this case, the transition point signals the temperature at which the central layers start to melt. In the limit of weak surface anchoring $W_0<W_0^*$, we observe that $T_c(N)$ decreases as the thickness is reduced. In this case, the surface layers have a weaker nematic order than the internal ones. The transition point represents the melting of the smectic order along the entire film, leading to its rupture. The characteristic anchoring W_0^* thus represents the physical situation at which the surface-induced ordering and the finite thickness effects are perfectly balanced, resulting in a thickness-independent transition temperature. Although the thickness dependence of the transition temperature becomes more pronounced when the parameter α is increased, the characteristic surface anchoring $W_0^*/V_0\simeq 0.25$ is roughly independent of α.

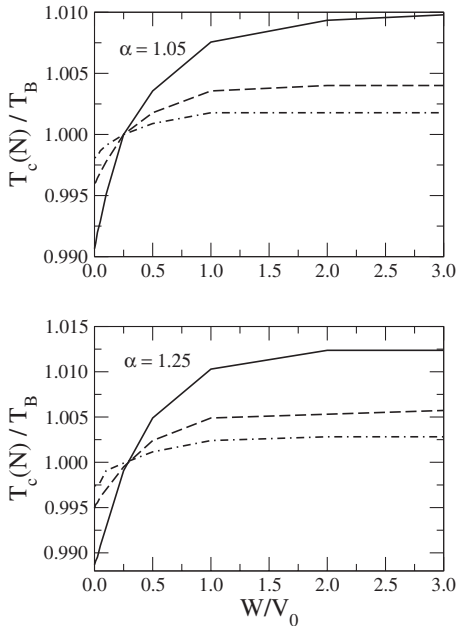

FIG. 4. Transition temperature $T_c(N)$ as function of the surface anchoring for different film thicknesses. Results for two representative values of the parameter α are shown: $\alpha=$ (a) 1.05 and (b) 1.25. $N=25$ (solid line), 50 (dashed line), and 100 (dot-dashed line). Notice the characteristic surface anchoring at which the transition temperature equals the bulk transition temperature irrespective of the film thickness.

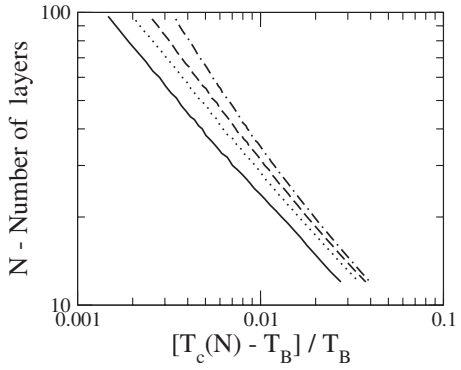

FIG. 5. Temperature dependence of the layer-thinning transition for different values of the parameter α: $\alpha=1.05$ (solid line), 1.25 (dotted line), 1.5 (dashed line), and 2.0 (dot-dashed line). We used $W_0=3V_0$. We can see that the exponent ν varies continuously along the thinning transition.

B. Sequence of layer-thinning transitions

In the limit of strong surface anchoring, our results can be interpreted in the context of layer-thinning transitions. When the temperature exceeds $T_c(N)$, the internal layers of the film undergo a discontinuous smectic-isotropic transition. The melted internal layers are expelled to the meniscus, which acts as a particle reservoir. As a result, the remaining film has its thickness reduced. After the thinning, the state at which the smectic order persists at the film center may remain as the most stable due to the predominance of the surface-induced ordering in this regime. An additional temperature increase is required to promote the melting of the remaining layers. Therefore, the film thickness will present a sequence of thinning transitions up to a temperature high enough to melt the entire film.

In Fig. 5, we plot the film thickness as a function of the reduced temperature $t=[T_c(N)-T_B]/T_B$, for different values of the parameter α. Our results do not follow a Kelvin law behavior for the temperature dependence of the thinning transition [33]. In fact, we observe that the data follow closely a power-law relation which is given by

$$N = N_0\left(\frac{T_c(N) - T_B}{T_B}\right)^{\nu}. \tag{11}$$

Here, N_0 is a fitting parameter. The exponent ν, which is given by the slope of the transition line in log-log scale, presents a small variation along the thinning transition. The slope becomes smaller as the layer-thinning transition proceeds. The range of values for the effective exponent depends on the parameter α. In particular, we observe that the average value of the exponent ν increases with α. It is important to recall that it is necessary to provide more thermal energy to destroy the smectic order for large α [35]. Table I summarizes the range of ν obtained from Fig. 5. The variability of the exponent ν with the parameter α is in good agreement with the experimental data, which are summarized in Table II. This result indicates that the presently used mean-field description seems to contain the essential ingredients needed to understand the physical mechanism leading to the layer-thinning transition. Further, it can provide a quantitative description for the relation between the transition temperature and the film thickness.

TABLE I. The bulk transition temperature T_B and the average exponent ν characterizing the layer-thinning transition for distinct values of the parameter α. The error bars account for the small variability of the exponent along the transition line in the range of film thicknesses shown in Fig. 5.

α	k_BT_B/V_0	ν
1.05	0.224 82	0.72 ± 0.04
1.25	0.240 85	0.74 ± 0.04
1.50	0.262 48	0.78 ± 0.04
2.00	0.307 84	0.86 ± 0.06

TABLE II. Experimental values of the exponent ν characterizing the layer-thinning transition. The range of experimental values is compatible with the present mean-field results. Sm*A*-*I* means the smectic-*A*–isotropic transition and Sm*A*-*N* the smectic-*A*–nematic transition.

Compound	Thinning transition	ν
54COOBC [27][a]	First-order Sm*A*-*I*	0.52
F3MOCPF6H5OB [29][b]	First-order Sm*A*-*I*	0.61 ± 0.04
H8F(4,2,1)MOPP [28][c]	First-order Sm*A*-*I*	0.70 ± 0.04
H10F5MOPP [24][d]	First-order Sm*A*-*I*	0.74 ± 0.02
8CB [30][e]	Weak first-order Sm*A*-*N*	0.69 ± 0.05
5O.6 [28][f]	Weak first-order Sm*A*-*N*	0.82
7AB [25][g]	Second-order Sm*A*-*N*	0.68 ± 0.03

[a]n-pentyl-4–n-pentanoyloxbiphenyl-4–carboxylate. This compound presents an irregular layer-thinning transition and the reported exponent has low confidence.
[b]4–(2, 2, 3, 3,4, 4, 4–heptafluorobutyloxcarbonyl)phenyl-4– [(n-perfluorehexyl) decyloxy] benzoate
[c]2– (4– (1,1–dihydro-2- (2-perfluorobutoxy-perfluoroethoxy) perfluoroethoxy)) phenyl-5–octylpyrimidine
[d]5–n-decyl-2–[4–n-(perfluoropentyl-methyleneoxy)phenyl] pyrimidine
[e]4–n-octyl-4'-cyanobiphenyl
[f]4–n-penthyloxybenzylidene-4–n-hexylaniline. In this compound, the layer-thinning transition was not observed in experiments with film diameters larger than 3 mm [28]. The error bars in ν were not reported for these two experiments.
[g]4,4'-diheptylazoxbenzene

IV. SUMMARY AND CONCLUSIONS

In conclusion, we investigated the interplay between surface anchoring and finite thickness effects on free-standing smectic films during the smectic-isotropic phase transition. Using an extended McMillan model [33], we obtained the profile of the nematic and smectic order parameters. By solving the self-consistent equations for the order parameter profiles and selecting the solution corresponding to the global minimum of the Helmholtz free energy, we observed that there is a characteristic strength of the surface anchoring de-

limiting two clearly distinct regimes of weak and strong anchoring. At weak anchoring the surface layers are less ordered than the internal ones. The transition temperature of films with a finite number of layers is below the bulk transition temperature T_B. This transition corresponds to the melting of the smectic order along the entire film. In the strong surface anchoring regime, the smectic order remains stable above the bulk transition temperature with the surface layers being more ordered than the internal ones. The transition temperature $T_c(N)$ presents a monotonic dependence on the surface anchoring. Nevertheless, $T_c(N)$ converges to a constant in the limit of $W_0/V_0 \to \infty$, due to the fact that the surface penetration length stays finite at a first-order transition.

At strong anchoring, the smectic-isotropic transition corresponds to the smectic order melting just at the central layers. This is the typical scenario of the layer-thinning transition experimentally found to occur in a series of compounds. After melting, the internal layers are expelled to the meniscus formed at the border of the hole over which the free-standing smectic film is spread. The ordered layers thus form a thinner smectic film that remains stable until a temperature high enough to promote further melting. This process continues through a sequence of layer-thinning transitions until the whole film is melted. Within the present mean-field approach, we have been able to reproduce the typical experimentally observed relation between the film thickness and the layer-thinning transition temperature. In particular, we showed that the film thickness has an effective power-law dependence on the temperature difference from the bulk transition temperature. The power-law exponent ν was found to present a weak dependence on the parameter α which is associated with the alkyl chain length of the liquid crystal molecule [35]. The range of values for ν that we obtained in our mean-field analysis is compatible with the values experimentally reported for the layer-thinning transition in distinct compounds. We would like to stress that the temperature dependence of the surface tension in fluorinated compounds was recently shown to be well reproduced by an extended McMillan theory [37,41,42]. In addition, the present work suggests that the layer-thinning transition may also be qualitatively and quantitatively well described within the scope of a mean-field theory. However, some questions still remain open, such as the possible connection between the formation of dislocation loops and the discontinuous reduction of the order parameter at $T_c(N)$ [31].

ACKNOWLEDGMENTS

We would like to thank CAPES, CNPq, Rede Nanobioestruturas, and FINEP (Brazilian Research Agencies), as well as FAPEAL (Alagoas State Research Agency) for partial financial support.

[1] W. H. de Jeu, B. I. Ostrovskii, and A. N. Shalaginov, Rev. Mod. Phys. **75**, 181 (2003).
[2] C. Barh, Int. J. Mod. Phys. B **8**, 3051 (1994).
[3] B. Jerome, Rep. Prog. Phys. **54**, 391 (1991).
[4] S. Heinekamp, R. A. Pelcovits, E. Fontes, E. Y. Chen, R. Pindak, and R. B. Meyer, Phys. Rev. Lett. **52**, 1017 (1984).
[5] B. M. Ocko, A. Braslau, P. S. Pershan, J. Als-Nielsen, and M. Deutsch, Phys. Rev. Lett. **57**, 94 (1986).
[6] J. Als-Nielsen, F. Christensen, and P. S. Pershan, Phys. Rev. Lett. **48**, 1107 (1982).
[7] R. Lucht, P. Marczuk, C. Bahr, and G. H. Findenegg, Phys. Rev. E **63**, 041704 (2001).
[8] C. C. Huang, I. M. Jiang, A. J. Jin, T. Stoebe, R. Geer, and C. Dasgupta, Phys. Rev. E **47**, 2938 (1993).
[9] C. Y. Chao, C. R. Lo, P. J. Wu, T. C. Pan, M. Veum, C. C. Huang, V. Surendranath, and J. T. Ho, Phys. Rev. Lett. **88**, 085507 (2002).
[10] R. Geer, T. Stoebe, and C. C. Huang, Phys. Rev. B **45**, 13055 (1992).
[11] D. Schlauf, Ch. Bahr, M. Glogarová, M. Kašpar, and V. Hamplová, Phys. Rev. E **59**, 6188 (1999).
[12] A. M. Somoza, L. Mederos, and D. E. Sullivan, Phys. Rev. Lett. **72**, 3674 (1994).
[13] A. M. Somoza, L. Mederos, and D. E. Sullivan, Phys. Rev. E **52**, 5017 (1995).
[14] J. V. Selinger and D. R. Nelson, Phys. Rev. A **37**, 1736 (1988).
[15] R. Lucht, C. Bahr, and G. Heppke, Phys. Rev. E **62**, 2324 (2000).
[16] R. Lucht and C. Bahr, Phys. Rev. Lett. **78**, 3487 (1997).
[17] T. Moses, Phys. Rev. E **64**, 010702(R) (2001).
[18] D. Beaglehole, Mol. Cryst. Liq. Cryst. **89**, 319 (1982).
[19] R. Lucht, C. Bahr, and G. Heppke, J. Phys. Chem. B **102**, 6861 (1998).
[20] L. V. Mikheev, Zh. Eksp. Teor. Fiz. **96**, 632 (1989)[Sov. Phys. JETP **69**, 358 (1989)].
[21] I. N. de Oliveira and M. L. Lyra, Phys. Rev. E **65**, 051711 (2002).
[22] I. N. de Oliveira and M. L. Lyra, Phys. Rev. E **70**, 050702(R) (2004).
[23] I. N. de Oliveira, M. L. Lyra, and L. V. Mirantsev, Phys. Rev. E **73**, 041703 (2006).
[24] T. Stoebe, P. Mach, and C. C. Huang, Phys. Rev. Lett. **73**, 1384 (1994).
[25] E. A. Mol, G. C. L. Wong, J. M. Petit, F. Rieutord, and W. H. de Jeu, Physica B **248**, 191 (1998).
[26] E. I. Demikhov, V. K. Dolganov, and K. P. Meletov, Phys. Rev. E **52**, R1285 (1995).
[27] A. J. Jin, M. Veum, T. Stoebe, C. F. Chou, J. T. Ho, S. W. Hui, V. Surendranath, and C. C. Huang, Phys. Rev. E **53**, 3639 (1996).
[28] P. M. Johnson, P. Mach, E. D. Wedell, F. Lintgen, M. Neubert, and C. C. Huang, Phys. Rev. E **55**, 4386 (1997).
[29] S. Pankratz, P. M. Johnson, H. T. Nguyen, and C. C. Huang, Phys. Rev. E **58**, R2721 (1998).
[30] F. Picano, P. Oswald, and E. Kats, Phys. Rev. E **63**, 021705 (2001).
[31] S. Pankratz, P. M. Johnson, R. Holyst, and C. C. Huang, Phys. Rev. E **60**, R2456 (1999).

[32] Y. Martínez-Ratón, A. M. Somoza, L. Mederos, and D. E. Sullivan, Phys. Rev. E **55**, 2030 (1997).
[33] L. V. Mirantsev, Phys. Lett. A **205**, 412 (1995).
[34] E. E. Gorodetsky, E. S. Pikina, and V. E. Podneks, Zh. Eksp. Teor. Fiz. **115**, 61 (1999) [JETP **88**, 35 (1999)].
[35] W. L. McMillan, Phys. Rev. A **4**, 1238 (1971).
[36] P. V. Dolganov, P. Cluzeau, G. Joly, V. K. Dolganov, and H. T. Nguyen, Phys. Rev. E **72**, 031713 (2005).
[37] M. Veum, E. Kutschera, N. Voshell, S. T. Wang, S. L. Wang, H. T. Nguyen, and C.C. Huang, Phys. Rev. E **71**, 020701(R) (2005).
[38] P. G. de Gennes and J. Prost, *The Physics of Liquid Crystals* (Clarendon Press, Oxford, 1993).
[39] A. A. Sonin, *The Surface Physics of Liquid Crystals* (Gordon and Breach Publishers, New York, 1995).
[40] D. E. Sullivan and A. N. Shalaginov, Phys. Rev. E **70**, 011707 (2004).
[41] L. V. Mirantsev, Phys. Rev. E **63**, 061701 (2001).
[42] M. Veum, M. K. Blees, N. Voshell, H. T. Nguyen, and C. C. Huang, Phys. Rev. E **74**, 011703 (2006).